Influence of surface treatment on the smectic ordering within porous glass

S. Kralj,[1,2] A. Zidanšek,[1] G. Lahajnar,[1] S. Žumer,[1,3] and R. Blinc[1,3]
[1]*J. Stefan Institute, Jamova 39, 1000 Ljubljana, Slovenia*
[2]*Department of Physics, Faculty of Education, University of Maribor, Koroška 160, 2000 Maribor, Slovenia*
[3]*Department of Physics, Faculty of Mathematics and Physics, University of Ljubljana, Jadranska 19, 1000 Ljubljana, Slovenia*
(Received 24 January 2000)

The influence of the surface treatment on the Sm-*A*–*N* phase transition of the 8CB (octylcyanobiphenyl) liquid crystal confined to controlled pore glass (CPG) matrices is studied. The characteristic linear size of voids in the chosen CPG matrix is 0.2 μm. The voids' surface was either nontreated or silane treated enforcing tangential or homeotropic anchoring, respectively. In both cases the x-ray measurements reveal a qualitative change of the temperature dependence of the smectic order-parameter correlation length in comparison to the bulk sample. In addition, the apparent smectic pretransitional ordering is observed for the silane-treated sample. A theoretical description based on the Landau-de Gennes type approach is developed to explain the experimental data. The surface positional anchoring strength of the silane-treated sample is estimated to be of the order of 10^{-4} J/m^2 and at least 100 times weaker for the nontreated case.

PACS number(s): 64.70.Md, 76.60.−k

I. INTRODUCTION

Smectic-*A* (Sm-*A*) liquid crystals (LC) are the least ordered phase of all smectic mesophases. A typical representative [1] consists of a stack of equally spaced layers of molecules aligned along the layer normal. The interlayer interactions are weak as compared to the interlayer interactions. Consequently the Sm-*A* phase exhibits two-dimensional (2D) liquidlike behavior in the layer plane and a 1D solidlike one along the stratification direction. In recent years there has been an increasing interest for the study of confined Sm-*A* in different nontrivial geometries [2] making use of the extreme sensitivity [1,3] of smectic positional ordering on surface induced perturbations. These studies reveal unanswered questions concerning the influence of surface phenomena (anchoring, wetting), finite-size effects, and randomness on thermodynamic properties of a confined system. Apart from simple planar and cylindrical confinements (e.g., anopore membranes [4]) controlled-pore glasses (CPG) [5], millipore membranes [6], or aerogels [7,8] are often used. Experimental studies reveal dramatic changes (e.g., change of critical behavior, temperature shift, or even cancellation of the bulk *N*–Sm-*A* phase transition) in comparison to the bulk behavior as the typical linear cavity size R approaches the smectic correlation length ξ. It has been shown that in confining matrices with a relatively strong geometrically induced disorder (high-density aerogels [7,8], millipore membranes [6]) randomness plays a dominant role. Less is known in cases with a weak but finite degree of randomness [3,9,10] realized, e.g., in CPG matrices. Several theoretical studies predict a disappearance of the bulk Sm-*A* quasi-long-range positional order even for weak geometrically induced disorder [3,9,10]. Consequently a new thermodynamically stable phase (the so-called Bragg glass phase [9,10]) is predicted. In addition pretransitional (wetting) phenomena are expected [11–17] if the coupling between the smectic density wave and the surface potential is strong enough.

In order to contribute to the understanding of some of these open questions, we decided to study the phase behavior of nematic and smectic liquid crystals confined to CPG matrices. In previous studies [5,18] we analyzed hysteresis phenomena, influence of confinement size, and surface treatment on the phase behavior of *n*CB LC ($n=5,8$) using deuterium nuclear magnetic resonance. With this technique an effective nematic degree of ordering can be inferred from the absorption spectrum. It can only yield indirect information on smectic ordering due to the coupling between smectic and nematic degrees of freedom [19,20]. But as shown in Ref. [18] this coupling allows only rough estimates of smectic ordering in CPG samples. For a better determination of smectic ordering, a method is needed that directly probes smectic layers. For this purpose we present, in this paper, an x-ray study of the evolution of the smectic A ordering of the 8CB (octylcyanobiphenyl) liquid crystal confined to a controlled-pore glass of a typical effective void radius $R=0.2\,\mu$m. In the experiment the CPG void's surface was either nontreated or treated with silane. We focus on the temperature evolution of the smectic correlation length and the pretransitional smectic partial wetting observed in the silane-treated sample. Some preliminary results of this paper were published in Ref. [21].

The outline of the paper is as follows. In Sec. II we present the experimental setup and measurements. In Sec. III the theoretical background is given. The results are discussed in Sec. IV and a possible role of dislocations in Sec. V. The conclusions are summarized in Sec. VI.

II. EXPERIMENT

A CPG matrix consists of voids resembling [22] curved cylinders. The cross section of voids is roughly spherical with well-defined effective radius R. The voids are randomly interconnected and curved. The average distance R_i between adjacent interconnections and the average curvature radius R_c is larger but roughly of the same order as R (i.e., typically $1<R_c/R<10$ and $1<R_i/R<R_c/R$). The voids surface is smooth even on the nm scale [18]. It is believed [18,22] that the nontreated CPG voids' surface enforces LC molecules to

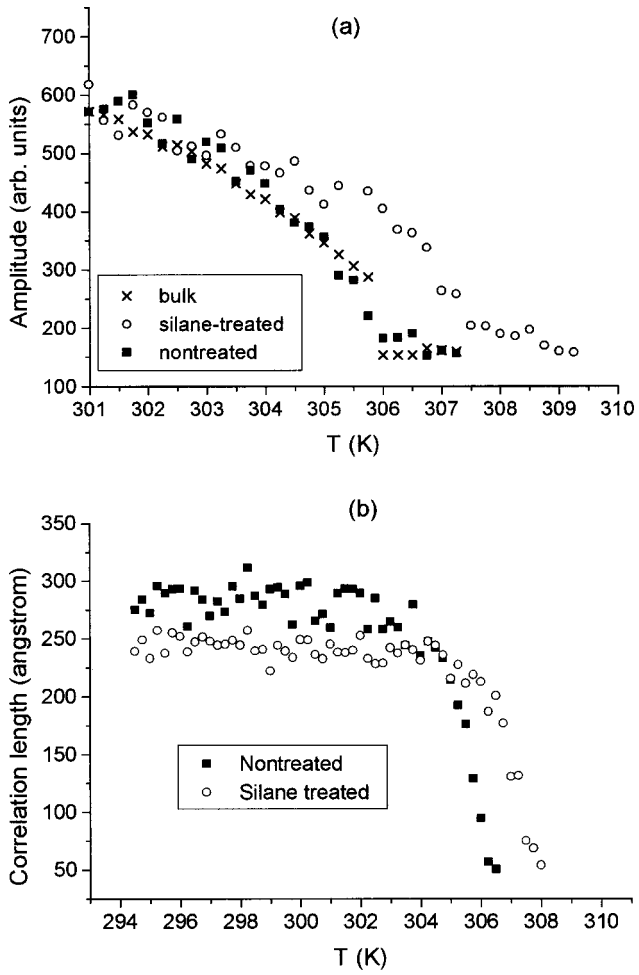

FIG. 1. Temperature evolution of the smectic ordering. (a) $\eta = \eta(T)$, (b) $\xi = \xi(T)$.

lie in its plane (the so-called tangentional anchoring [23]). The corresponding orientational anchoring strength is estimated [5] to be larger than 10^{-5} J/m^2.

In our paper we used CPG matrices with a monodispersed radius $R = (200 \pm 20)$ nm. The voids' surface was either nontreated or silane treated. The silane coating is known to enforce relatively strong homeotropic anchoring [18] in which molecules tend to orient along the surface normal.

We measured a small angle x-ray scattering pattern of the bulk, silane-treated and nontreated sample between 20 and 50 °C at the Austrian small angle x-ray scattering beamline of the Elettra Synchrotrone in Trieste [24]. A smectic peak was observed at the inverse distance between the smectic layers in the smectic A phase. The amplitude of this peak is proportional to the average degree of smectic ordering in the observed sample. When the line shape is fitted to a Lorentzian, the linewidth reveals the smectic correlation length ξ of the confined liquid crystal, and the position of the line gives the distance between the neighboring smectic layers [7].

In Fig. 1(a) we show the temperature evolution of the smectic degree of ordering for the nontreated, silane-treated and bulk sample. The amplitude η of smectic ordering is given in arbitrary units. The qualitative temperature dependencies of the order parameter $\eta = \eta(T)$ in the bulk and in the nontreated sample are similar. The silane-treated sample clearly shows smectic pretransitional phenomena. The temperature dependence of the smectic correlation length [Fig. 1(b)] in both confined samples dramatically departs from the bulk behavior.

III. THEORY

A. Free energy

In order to describe the observed behavior, we use the Landau–de Gennes type phenomenological approach. The orientational ordering within layers is given by the uniaxial nematic director field **n** pointing along the local average orientation of rodlike LC molecules. In the Sm-*A* phase **n** tends to be aligned along the layer normal. Because in our case the temperature interval of the stable bulk Sm-*A* phase is well below the nematic-isotropic phase transition, we can safely assume a constant value of the nematic orientational order parameter [25].

We describe the smectic degree of ordering with the complex smectic order parameter $\psi = \eta e^{i\phi}$. The smectic positional order parameter η determines the degree of smectic ordering and the phase factor ϕ, the position of smectic layers. In this single harmonic approximation [1,26] ψ is related to the molecular density σ as $\sigma = \sigma_0(1 + \psi + \psi^*)$, where σ_0 determines the mean density of the smectic.

In terms of these continuum fields we express the free energy of a Sm-*A* phase as [1,27,28]

$$F = \int \int_{\Omega} \int (f_e^{(n)} + f_h^{(s)} + f_e^{(s)}) d^3r + \int_{\delta} \int_{\Omega} (f_a^{(n)} + f_a^{(s)}) d^2r, \tag{1}$$

where $\delta\Omega$ determines the boundary of the confining volume Ω. The quantities $f_j^{(i)}$ stand for the free-energy densities where the superscript i determines either the nematic (n) or smectic (s) component and the subscript j determines the elastic (e), the homogeneous (h), or the surface anchoring (a) contribution.

The nematic elastic term, expressed in the single elastic constant K approximation as

$$f_e^{(n)} = \frac{K}{2}[(\nabla \cdot \mathbf{n})^2 + (\nabla \times \mathbf{n})^2] \tag{2a}$$

tends to enforce homogeneous orientational ordering.

The amplitude of the smectic order parameter in the unconstrained Sm-*A* LC is determined by the homogeneous smectic term

$$f_h^{(s)} = a_0 \frac{T - T_{NA}}{T_{NA}} \eta^2 + \frac{b}{2} \eta^4. \tag{2b}$$

The quantities a_0, b are the material constants and T_{NA} is the temperature of the bulk continuous *N*–Sm-*A* phase transition.

The smectic elastic term

$$f_e^{(s)} = C_{\parallel} |(\mathbf{n} \cdot \nabla - iq_0)\psi|^2 + C_{\perp} |(\mathbf{n} \times \nabla)\psi|^2 \tag{2c}$$

consists of compressibility and bending terms weighted with the smectic elastic constants $C_{\parallel}$ and $C_{\perp}$ respectively. These terms tend to enforce the equilibrium layer spacing d_0

$=2\pi/q_0$ and to align **n** along the smectic layer normal. Henceforth we neglect the anisotropy of the smectic elastic constants, i.e., $C \equiv C_\perp = C_\parallel$.

The nematic surface orientational term tends to align **n** along the easy axis $\mathbf{e}_s$ at the boundary. In the lowest-order approximation it is written as [23,29]

$$f_a^{(n)} = \frac{W_n}{2}[1-(\mathbf{n}\cdot \mathbf{e}_s)^2], \tag{3a}$$

where W_n measures the surface orientational anchoring strength.

The smectic positional anchoring term is modelled by a simple contact coupling including up to quadratic terms in order parameter [30]

$$f_a^{(s)} = \frac{W_s}{2}|\psi-\psi_s|^2. \tag{3b}$$

It is characterized by the positional anchoring strength W_s and the preferred smectic ordering ψ_s at the surface.

B. Characteristic lengths

The most important characteristic lengths [1] of the unconstrained bulk Sm-*A* LC are related to the decay length of perturbations in the nematic and smectic order. The smectic order parameter correlation length is given by

$$\xi = \sqrt{\frac{C}{\frac{1}{2}[\partial^2 f_h^{(s)}/\partial \eta^2]}}. \tag{4a}$$

It estimates the distance over which locally perturbed smectic degree of ordering vanishes. Above T_{NA} one finds

$$\xi = \sqrt{\frac{C}{a_0(T-T_{NA}/T_{NA})}} = \frac{\xi_0}{\sqrt{T-T_{NA}/T_{NA}}},$$

where $\xi_0 = \sqrt{C/a_0}$ describes the bare smectic correlation length. The nematic penetration length is defined as

$$\lambda = \sqrt{\frac{K}{2C\eta_b^2 q_0^2}}, \tag{4b}$$

where

$$\eta_b = \sqrt{\frac{a_0(T_{NA}-T)}{bT_{NA}}}$$

stands for the bulk smectic order parameter. The penetration length estimates the distance over which the locally induced perturbation in nematic orientational ordering vanishes. Both lengths ξ and λ diverge at the continuous bulk *N*–Sm-*A* phase transition. Deep in the Sm-*A* phase their value is typically of order of 1 nm. The ratio ξ/λ distinguishes between type I and type II Sm-*A* phases [1]. In the type II phase, characterized roughly by $\xi/\lambda > 1$, a network of dislocations can be stabilized if subjected to an external stress in contrast to the type I phase. The results of this and previous studies [8,18] indicate that the 8 CB smectic-*A* phase is of type II.

Confining the system to a cavity introduces into the model additional typical lengths. The geometry of the problem is described in terms of the effective void cross section radius *R*, the average distance between intersections R_i and the average curvature R_c of voids. For $R/\xi \gg 1$, the system on the average exhibits more or less a bulklike behavior. For *R* approaching the value of ξ, the effects of confinement (i.e., finite-size effects, surface phenomena, confinement induced randomness) are increasingly manifested.

In addition the interactions at the LC-substrate interface introduces the orientational [1] and positional [1,30] anchoring extrapolation lengths

$$d_e^{(n)} = \frac{K}{W_n}, \quad d_e^{(s)} = \frac{C}{W_s}, \tag{4c}$$

respectively. In the regime $R/d_e^{(n)} > 1$ and $R/d_e^{(s)} > 1$ the influence of surface orientational and positional anchoring becomes important, respectively.

C. Scaling and parametrization

For convenience we introduce the scaled smectic order parameter $\varepsilon = \eta/\eta_0$, where η_0 describes the saturated value of η [i.e., $\eta_0 = \eta(T=0)$]. The distances are scaled in units of *R*, where *R* is a typical linear length in the direction perpendicular to the limiting boundary (i.e., in our case equals the effective radius of CPG voids). With this renormalization we obtain the following expression for the dimensionless free energy $G = F/(RC\eta_0^2)$:

$$\begin{aligned} G = \int \int_Q \int d^3\mathbf{x} \Bigg\{ & \frac{K}{2\eta_0^2 C}[(\boldsymbol{\nabla}'\cdot\mathbf{n})^2 + (\boldsymbol{\nabla}'\times\mathbf{n})^2] \\ & + \frac{R^2}{\xi_0^2}\left(\tau\varepsilon^2 + \frac{\varepsilon^4}{2}\right)\Bigg\} + \int \int_\Omega \int d^3\mathbf{x}\{\varepsilon^2[(\mathbf{n}\cdot\boldsymbol{\nabla}'\Phi \\ & - q_0 R)^2 + (\mathbf{n}\times\boldsymbol{\nabla}'\Phi)^2] + (\mathbf{n}\cdot\boldsymbol{\nabla}'\varepsilon)^2 + (\mathbf{n}\times\boldsymbol{\nabla}'\varepsilon)^2\} \\ & + \int_\delta \int_O d^2\mathbf{x}\Bigg(\frac{R}{2d_e^{(n)}}\frac{K}{\eta_0^2 C}[1-(\mathbf{n}\cdot e_s)^2] \\ & + \frac{R}{2d_e^{(s)}}|\varepsilon e^{i\phi} - \varepsilon_s e^{i\Phi_s}|^2\Bigg). \end{aligned} \tag{5}$$

Here $\boldsymbol{\nabla}'$ stands for the dimensionless nabla operator, $\tau = T - T_{NA}/T_{NA}$ is the reduced temperature, and ε_s is the scaled smectic order parameter preferred by the surface. In this scaling the relative importances of different terms as functions of *R* are clearly visible. Note that the spatial variations in ϕ and **n** typically evolve overall the available phase space. On the other hand, ε varies over a distance given by ξ.

We originate from expression Eq. (5) to study pretransitional smectic ordering numerically. For a particular model of a CPG matrix, we will use appropriate ansatzs for the nematic director field and positions of smectic layers. The spatial variation of ε is then obtained numerically solving the Euler-Lagrange equation resulting from the minimization of *G*.

IV. TEMPERATURE EVOLUTION OF THE SMECTIC ORDERING

A. Pretransitional effects

We assume that the main characteristics can be inferred from a simple toy model of the CPG matrix. For this purpose we chose an infinite cylinder of radius R. The walls of the cylinder enforce either tangential or homeotropic anchoring. These cases reasonably simulate the orientational anchoring conditions for both the nontreated (tangentional) and silane-treated (homeotropic) CPG sample.

For tangential anchoring the smectic layers are stacked along the cylinder axis. In this case the coupling between the smectic layers and the surface is relatively weak [31] and consequently no pretransitional effects are expected in line with experimental results.

On the contrary, for homeotropic anchoring the coupling between smectic layers and the surface can be relatively strong leading to pretransitional phenomena. The prerequisite for this is a strong enough orientational anchoring with respect to nematic elastic forces: i.e., $R/d_e^{(n)}>0$. In order to estimate the surface positional anchoring strength necessary for observable prewetting phenomena, we select a radial director field profile within the cylinder. The smectic order parameter is expected to vary only along the radial direction characterized by the coordinate ρ of the cylindrical coordinate system [i.e., $\varepsilon=\varepsilon(\rho)$]. This yields a line dislocation at the cylinder axis prohibiting smectic ordering for all temperatures. Below T_{NA} the smectic periodicity is assumed to be equal to q_0.

In a real situation the director profile is probably different [28] from the above one at least above T_{NA}. More likely the escaped radial-like [32] profile is realized where strong variations are restricted to the narrow region at the cylinder axis. In this configuration the nematic director field gradually reorients from the radial direction at the surface into the direction along the symmetry axis at the center of the cylinder. Via this ''escape into the third dimension'' [32] the line singularity in **n** is avoided. From the smectic perspective both situations are similar. Since the phenomena of our interest take place at the surface we monitor the smectic ordering with $\varepsilon(1)=\varepsilon(\rho=1)$ describing ordering at the cylinder wall and with

$$\langle\varepsilon\rangle=2\int_0^1\varepsilon(\rho)\rho d\rho$$

yielding the average degree of smectic ordering in the cylinder.

With the above assumptions Eq. (5) simplifies to

$$G-G_n=\int_0^1\rho d\rho\left[\frac{R^2}{\xi_0^2}(\tau\varepsilon^2+\varepsilon^4)+\left(\frac{d\varepsilon}{d\rho}\right)^2\right]+\frac{R}{2d_e^{(s)}}[\varepsilon(1)-\varepsilon_s]^2. \quad (6)$$

Here G_n describes the nematic elastic free-energy contribution. The minimization of Eq. (6) yields the Euler-Lagrange equations for $\varepsilon(\rho)$, which are solved numerically using the relaxation method.

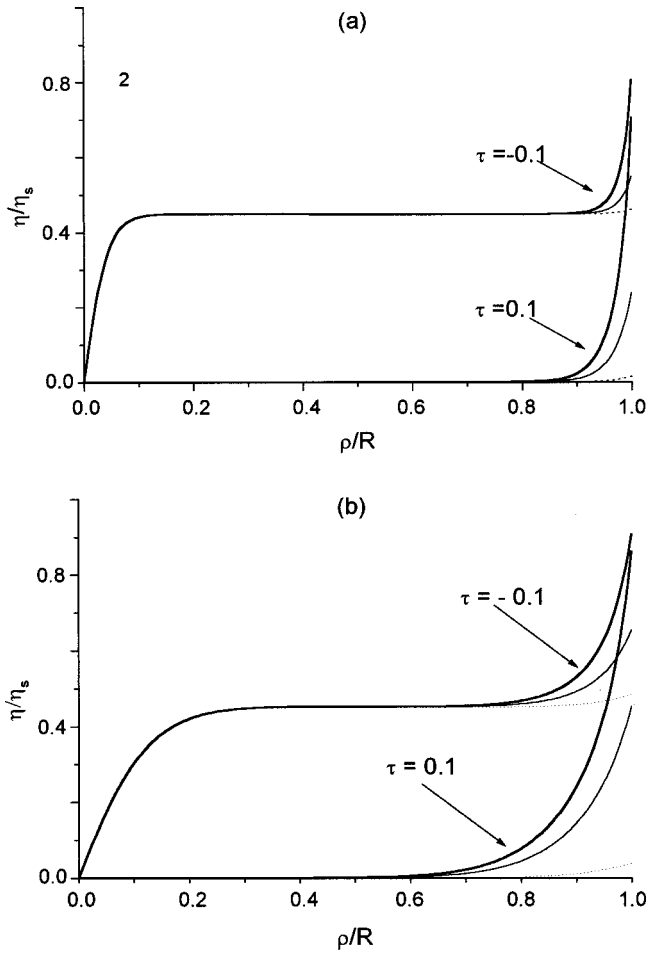

FIG. 2. The smectic order parameter spatial variation above ($\tau=0.1$) and below ($\tau=-0.1$) the bulk N–Sm-A phase transition for different surface positional anchoring strengths. $R/d_e^{(s)}=100$ (thick line), 10 (thin line), 1 (dotted line). (a) $(R/\xi_0)^2=10^4$, (b) $(R/\xi_0)^2=10^3$.

In Fig. 2 we show spatial profiles $\varepsilon=\varepsilon(\rho)$ for different values of R/ξ_0 and $R/d_e^{(s)}$ above ($\tau=0.1$) and below ($\tau=-0.1$) the bulk N–Sm-A phase transition. At the surface, the degree of ordering is increased because $R/d_e^{(s)}>0$ supports the smectic growth. Surface enhanced ordering extends over a distance roughly given by the bulk smectic correlation length. In the vicinity of the cylinder axis ($\rho=0$) the smectic melts because of strong nematic director field distortions.

In Fig. 3 we plot $\varepsilon(1)$ and $\langle\varepsilon\rangle$ as a function of τ for different ratios R/ξ_0 and $R/d_e^{(s)}$. In our CPG samples we have $R/\xi_0\approx10^2$. In such a case, the prewetting is evidently manifested in $\langle\varepsilon\rangle$, which can be determined using x-ray spectrometry, if $R/d_e^{(s)}>1$. The best fit to experimental results is shown in Fig. 3(c) yielding $R/d_e^{(s)}\approx100\pm10$.

B. Smectic correlation length

The x-ray measurements reveal a dramatically different dependence $\xi=\xi(T)$ in both confined samples as compared to the bulk behavior [Fig. 1(b)]. In the bulk, ξ measures the distance over which locally induced perturbations in the degree of smectic ordering persists. In its derivation it is assumed that ϕ adopts the equilibrium profile (i.e., $\phi=\phi_{TD}=q_0z$). It should be stressed that in the x-ray investigation

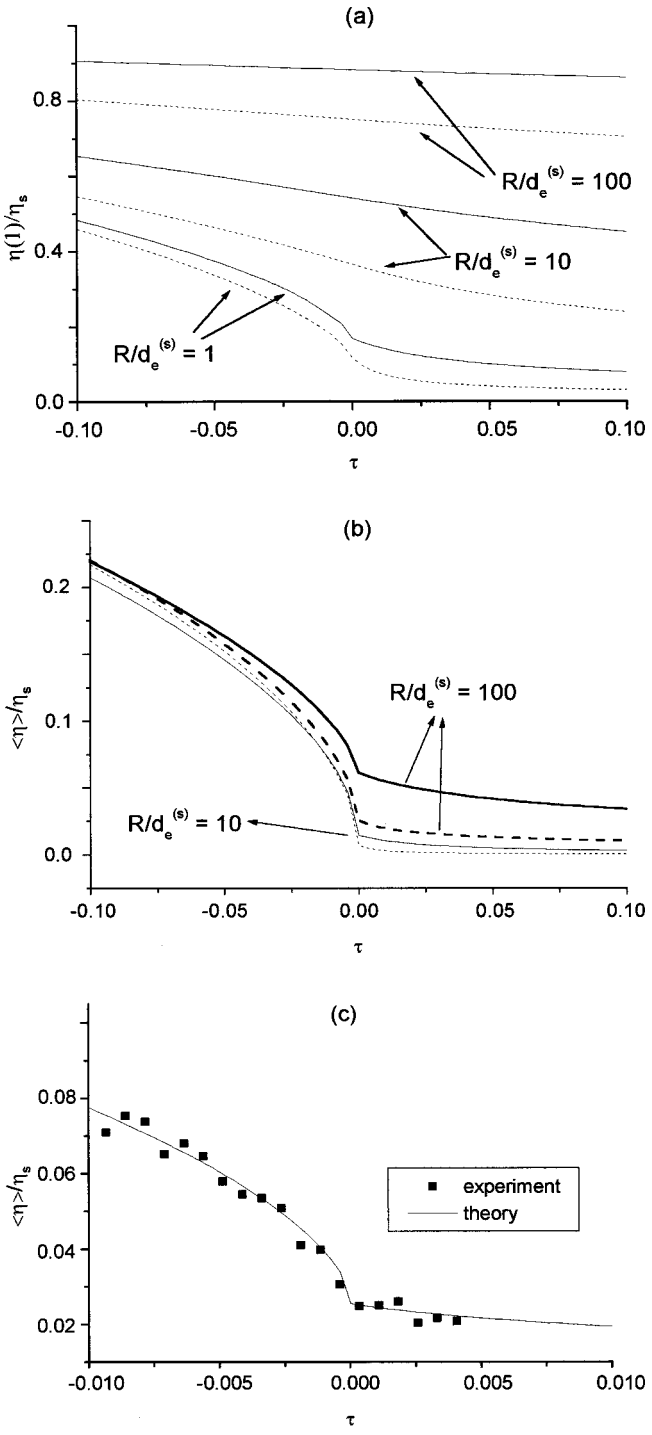

FIG. 3. The surface (a) and average (b) degree of smectic ordering as a function of τ for different surface positional strengths. Full line: $(R/\xi_0)^2=10^3$, dotted line: $(R/\xi_0)^2=10^4$. In (c) the best fit is shown obtained for $(R/\xi_0)^2=10^4$ and $R/d_e^{(s)}\approx 100$.

of the CPG samples, the correlation between smectic layers cannot neglect the effect of $\phi \neq \phi_{TD}$.

To explain qualitatively this effect, we first focus on Eqs. (1) and (5). The only terms including the phase factor are

$$f_\phi = C\eta^2[(\mathbf{n}\cdot\boldsymbol{\nabla}\Phi - q_0)^2 + (\mathbf{n}\times\boldsymbol{\nabla}\Phi)^2]. \tag{7}$$

Assuming homogeneous ordering in $\mathbf{n}$ and η, one sees that the Euler-Lagrange equation for ϕ does not contain any characteristic length. Thus if ϕ departs from its ground-state configuration, in which $f_\phi=0$, its deformation will spread over the whole available space occupied by the smectic phase. In the CPG samples, the most important perturbations affecting the phase are random curvatures and cavity interconnectedness [see Fig. 4(a)]. This causes f_ϕ to be different from zero and yields a dramatic change in the $\xi(T)$ behavior.

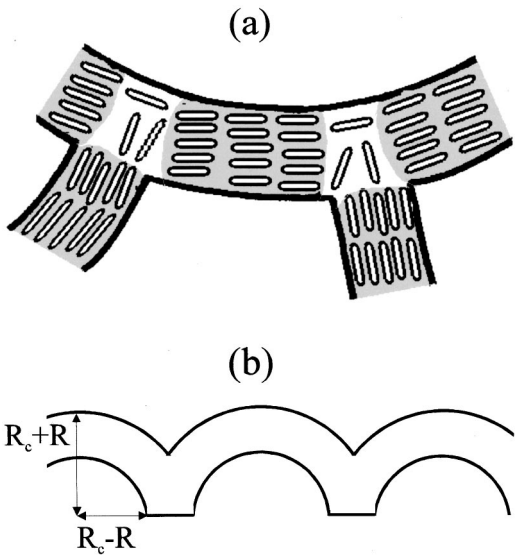

FIG. 4. (a) A schematic presentation of smectic domains (shadowed regions) in a nontreated CPG matrix. (b) The model geometry used to estimate the concentration of defects in CPG matrices.

In order to estimate this change we limit ourselves for the moment to the one-dimensional case where only variations along the z axis are allowed. We next assume that the phase factor departs from the bulk equilibrium layering due to the confinement, i.e., $\phi = q_0 z + \delta\phi$ where $\delta\phi = \delta\phi(z)$. Consequently above T_{NA} one obtains

$$f \approx a\eta^2 + C\left(\frac{d\eta(z)}{dz}\right)^2 + C\eta^2\left(\frac{d\delta\Phi(z)}{dz}\right)^2. \tag{8}$$

Based on the already described arguments we make the following approximation:

$$\frac{d\delta\Phi(z)}{dz} \approx \frac{\delta\Phi}{\xi_d}$$

where ξ_d describes the length of a typical smectic domain (i.e., a region exhibiting smectic ordering) and $\delta\phi<1$ is the change of $\delta\phi(z)$ across the domain. Thus the phase disturbance can be viewed as a renormalization of the coefficient in front of η^2 (i.e., $a \to a + C(\delta\Phi/\xi_d)^2$). Following the standard procedure of the correlation length [1] determination one finds the equation relating ξ and ξ_d:

$$\frac{1}{\xi^2} = \frac{a}{C} + \left(\frac{\delta\Phi}{\xi_d}\right)^2. \tag{9}$$

Well above T_{NA} the domain size ξ_d is in fact determined by the size of smectic clusters that temporarily appear due to random fluctuations, thus $\xi_d=\xi$. The upper value for ξ_d is R_d where R_d stands for the geometrically imposed domain

boundary. With this in mind and taking into account Eq. (9), one finds for the case $\xi_d < R_d$:

$$\xi \approx \sqrt{(C/a)(1-\delta\Phi^2)}, \tag{10a}$$

and in the opposite case

$$\xi \approx \frac{1}{\sqrt{a/C+\delta\Phi^2/R_d^2}}. \tag{10b}$$

One sees that at relatively high temperatures the correlation length in confined samples is reduced in comparison to the bulk case because of distortions that hinder smectic ordering. Close to T_{NA} we have $|a|/C \ll 1$ and consequently one gets $\xi \propto R_d$. On approaching the bulk phase transition, ξ saturates at R_d. Note that Eqs. (10) yield correct information only from a qualitative point of view above T_{NA}. Below T_{NA} the variational parameters ϕ and η are strongly coupled requiring a more detailed derivation.

In the CPG matrix the value of R_d depends on the anchoring condition that determines the direction of layer growth. For strong enough homeotropic orientational anchoring (i.e., $R/d_e^{(n)} > 1$) the layers grow from the surface towards the interior of a cavity. In this case we have $R_d \leqslant R$. For tangential anchoring R_d corresponds to an average distance between two adjacent void interconnections or sites of strong curvature. This is typically larger but comparable to R. This prediction is consistent with experimental findings showing that ξ for the silane-treated sample is smaller than ξ for the nontreated sample [Fig. 1(b)].

V. DISLOCATION NETWORK

In CPG matrices various and often contradicting perturbations enforce a finite concentration of topologically [33] stable (screw [1,34,35] or edge [1,30,34]) line dislocations in the ordering field ψ below T_{NA}. The corresponding network of defects has no long-range order because its main origin is randomness (introduced via voids' curvature and interconnections). The core of defects roughly extends over the linear size given by ξ. In the following we roughly estimate the role of dislocations on the global behavior in the silane-treated and nontreated sample.

A. Silane-treated sample

Let us assume that the condition $R/d_e^{(n)} > 1$ is fulfilled in the silane-treated sample so that the homeotropic anchoring is obeyed by LC molecules. Thus $W_n > 2.5 \times 10^{-5}$ J/m^2 (assuming $K \approx 5 \times 10^{-12}$ J/m, $R = 0.2\,\mu$m) must be realized. This is certainly true for the silane coating. [18] In the opposite case (e.g., in CPG matrices with $R \ll 1\,\mu$m) the resulting LC structure [28] is similar to that established in the nontreated sample that will be considered afterwards.

For the homeotropic surface orientation of LC molecules the curvature of voids only weakly affects the degree of smectic ordering. LC responds to voids' curvature with layer undulation involving mostly the nematic splay distortion. This is ''allowed'' in the smectic phase and does not force the system to form dislocations (note that in smectic LC in addition to topological also the geometrical requirements control the generation of defects in contrast to the nematic phase [36]).

In such a case the number of dislocations $N_d^{(i)}$ is roughly given by $N_d^{(i)} \approx L/R_i$, where L is the overall length of cylindrical voids, R_i is the average distance between interconnections, and index i denotes interconnections. Our previous study [18] indicates $R_i \propto R$ and $R_i > R$. The volume V_0 of essentially nematic ordering (i.e., $\eta \approx 0$) surrounding each line dislocation is $V_0 \approx \pi\xi^2 R$, where we assume that the length of dislocation is roughly R (i.e., it exists only at the interconnection whose size is roughly R). Thus the volume $V_d^{(i)}$ occupied by dislocations is

$$V_d^{(i)} \approx N_d^{(i)} V_0 \approx \frac{\pi L \xi^2 R}{R_i}.$$

The average smectic parameter of the sample can be expressed as

$$\langle \eta \rangle \approx \eta_b \frac{V_{\mathrm{LC}} - V_d}{V_{\mathrm{LC}}}, \tag{11}$$

where $V_{\mathrm{LC}} = \pi R^2 L$ is the volume occupied by LC and $V_d = V_d^{(i)}$ the volume occupied by defects. Taking this into account we obtain

$$\frac{\langle \eta \rangle}{\eta_b} \approx 1 - \frac{V_d}{V_{\mathrm{LC}}} \approx 1 - \frac{\xi^2}{R_i R}. \tag{12}$$

Close to the phase transition $\xi \approx R$ and deviations from bulk ordering are proportional to R/R_i. Note that each intersection does not necessary introduce a dislocation so that the effective value of R_i entering Eq. (11) is in fact larger. In addition, the average smectic order inside the dislocation core is different from zero. Thus close to the transition temperature the departures from the bulk behavior due to smectic dislocations is expected to be independent of R and of the order of a few percent. With decreased temperature the correlation length shrinks and departures from the bulk behavior gradually decrease.

For the homeotropic anchoring one expects melted smectic ordering at a void's symmetry axis. The resulting melted volume would be proportional to $V_d^{(m)} \approx L\pi\xi^2$, giving rise to a substantial drop in $\langle \eta \rangle$ at least close to T_{NA} which is experimentally not observed. A possible reason for this is that softening of the smectic ordering at the center is compensated by an increase of η at the surface that occupies relatively larger volume. This scenario is supported by the numerical simulation given in Sec. IV A [see Fig. 2(a)]. Another possibility is that the smectic phase locally finds another way to resolve elastic distortions at the center, which requires less melting.

B. Nontreated sample

The nontreated sample enforces tangentional orientational ordering. In this case the curvature of voids tends to locally compress or dilate smectic layers. This is ''forbidden'' in the smectic phase. Consequently the type I Sm-*A* LC would melt. In contrast the type II Sm-*A* LC, to which our Sm-*A* samples evidently belong, incorporates into the smectic or-

dering a network of dislocations. In this way the globally distributed stress is redistributed to finite regions (dislocations).

We next estimate the influence of curvature induced dislocations. We assume that the average void curvature is R_c as depicted in Fig. 4 and has the half-spherical shape. The total length of voids in a CPG matrix is then $L=N_{\rm arc}\pi R_c$, where $N_{\rm arc}$ determines the number of arcs. When the difference between the outer [determined by the radius R_c+R in Fig. 4(b)] and the inner void (the radius R_c-R) wall length along the void axis equals d_0, an edge dislocation has to be included. Thus on going along the void axis for distance πR_c (one arc) one encounters

$$N_d^{(c)}=\frac{\pi(R_c+R)-\pi(R_c-R)}{d_0}=q_0R$$

edge dislocations. Here the superscript (c) describes ''curvature'' induced dislocations. The volume that the core of each dislocation encompasses is $V_0\approx\pi\xi^2R_d$, where R_d is the length of the dislocation. Simple geometrical facts suggest $R_d<R$ and $R_d\propto R$. The volume of all curvature induced dislocations is then $V_d^{(c)}\approx N_d^{(c)}N_{\rm arc}V_0\approx L\xi^2Rq_0R_d/R_c$. To estimate the corresponding drop of smectic ordering we use Eq. (10) where $V_d\approx V_d^{(i)}+V_d^{(c)}$ yielding

$$\frac{\langle\eta\rangle}{\eta_b}\approx 1-\frac{\xi^2}{R_iR}-\frac{\xi^2q_0R_d}{R_cR}. \tag{13}$$

Thus, in this case, defects originate from random void interconnections and also from the random curvatures. As in the previous case the drop of smectic ordering is expected to be independent of R and of order of a few percent.

VI. CONCLUSIONS

We study the impact of CPG confining matrices on the temperature evolution of smectic-*A* LC ordering. We interpret the x-ray measurements of 8CB LC confined to the nontreated and silane-treated CPG matrix of the effective radius $R\approx 0.2\,\mu$m using the Landau–de Gennes phenomenological approach.

In the nontreated sample the tangential orientational anchoring is realized. The coupling between the smectic density wave and surface potential is relatively weak and consequently smectic pretransitional phenomena are not observed. The smectic order parameter temperature evolution roughly resembles the bulk $\eta=\eta(T)$ dependence. We expect that a relatively weak disorder originating from random cavity interconnections and curvatures introduces a disordered network of smectic dislocations into the system. Consequently the average smectic order parameter is believed to be reduced by a few percent.

In the silane-treated sample, the homeotropic orientational anchoring is realized. The surface positional coupling is in this case strong enough to cause pretransitional smectic ordering. The comparison of theoretical and experimental results suggests $R/d_e^{(s)}>1$. In this case the only source of numerous smectic dislocations are random void interconnections. On geometrical grounds one expects, in this case, the melted regions at the voids' symmetry axes.

In both confined samples the temperature dependence of the smectic correlation length dramatically departs from the bulk behavior. It gradually increases by lowering temperature from the nematic phase and saturates roughly at R for $T\ll T_{NA}$. For the nontreated sample the saturation value of ξ is larger as compared to the silane-treated sample. The observed behavior can be qualitatively understood in terms of our model assuming that local departures of ϕ from its bulk value are caused by void interconnections and curvatures.

Note that recent results [11–17] indicate extreme sensitivity of smectic prewetting phenomena on the LC-interface potential $W_{\rm int}$. This is in our approach modeled by a simple surface smectic positional anchoring term weighted with the anchoring constant W_p. More elaborate theoretical approaches [15] predict a finite number n of first-order layer transitions with increased $W_{\rm int}$ corresponding to partial wetting. For strong enough $W_{\rm int}$ a complete wetting regime can be realized via an infinite sequence of layer transitions. But in practice the high-n layer transitions are expected to be eliminated because of surface imperfections. In addition the wetting phenomena are highly sensitive to a type of LC molecules [11,12,15]. In order to explore in detail the expected rich smectic pretransitional phenomena and nonhomogenity of the smectic ordering, we plan to extend our study to CPG samples of different void sizes R and different members of the nCB homologous series using high-resolution calorimetry.

ACKNOWLEDGMENTS

We thank E. G. Virga, V. Popa-Nita, and L. Hazelwood for useful conversations. The research was supported by the Slovenian Ministry of Science and Technology (Grant No. J1-0595-1554-98) and bilateral project ''Structure and dynamics of defects in spatially restricted liquid crystals'' between Italy and Slovenia.

[1] P. G. de Gennes and J. Prost, *The Physics of Liquid Crystals* (Oxford University Press, Oxford, 1993).

[2] *Liquid Crystals in Complex Geometries Formed by Polymer and Porous Networks*, edited by G. P. Crawford and S. Žumer (Taylor & Francis, London, 1996).

[3] L. Radzihovsky and J. Toner, Phys. Rev. Lett. **78**, 4414 (1997); **79**, 4214 (1997).

[4] G. S. Iannacchione, J. T. Mang, S. Kumar, and D. Finotello, Phys. Rev. Lett. **73**, 2708 (1994).

[5] S. Kralj, A. Zidanšek, G. Lahajnar, S. Žumer, and R. Blinc, Phys. Rev. E **57**, 3021 (1998).

[6] S. Qian, G. S. Iannacchione, and D. Finotello, Phys. Rev. E **53**, R4291 (1996); **57**, 4305 (1998).

[7] T. Bellini, N. A. Clark, C. D. Muzny, L. Wu, C. Garland, D. W. Schaefer, and B. Olivier, Phys. Rev. Lett. **69**, 788 (1992).

[8] N. A. Clark, T. Bellini, R. M. Malzbender, B. N. Thomas, A. G. Rappaport, C. D. Muzny, D. W. Schaefer, and L. Hrubesh, Phys. Rev. Lett. **71**, 3505 (1993).

[9] M. J. P. Gingras (unpublished).
[10] B. Jacobsen, K. Saunders, L. Radzihovsky, and J. Toner, Phys. Rev. Lett. **83**, 1363 (1999).
[11] B. M. Ocko, A. Braslau, P. S. Persan, J. Als-Nielsen, and M. Deutsch, Phys. Rev. Lett. **57**, 94 (1986).
[12] B. M. Ocko, Phys. Rev. Lett. **64**, 2160 (1990).
[13] L. Moreau, P. Richetti, and P. Barois, Phys. Rev. Lett. **73**, 3556 (1994).
[14] Z. Pawlowska, T. J. Sluckin, and G. F. Kventsel, Phys. Rev. A **38**, 5342 (1988).
[15] A. M. Somoza, L. Mederos, and D. E. Sullivan, Phys. Rev. Lett. **72**, 3674 (1994).
[16] A. Sparavigna, G. Barbero, L. Komitov, P. Palffy-Muhoray, and A. Strigazzi, Mol. Cryst. Liq. Cryst. **251**, 231 (1994).
[17] A. Poniewierski and A. Samborski, Phys. Rev. E **51**, 4574 (1995).
[18] S. Kralj, A. Zidanšek, G. Lahajnar, I. Muševič, S. Žumer, R. Blinc, and M. M. Pintar, Phys. Rev. E **53**, 3629 (1996); S. Kralj, A. Zidanšek, G. Lahajnar, S. Žumer, and R. Blinc, *ibid.* **57**, 3021 (1998).
[19] R. Blinc, Liq. Cryst. **26**, 1295 (1999).
[20] P. Ziherl, Phys. Rev. E (to be published).
[21] A. Zidanšek, S. Kralj, R. Repnik, G. Lahajnar, M. Rappolt, H. Amenitsch, and S. Bernstorff, J. Phys. (to be published).
[22] M. D. Dadmun and M. Muthukumar, J. Chem. Phys. **98**, 4850 (1993).
[23] B. Jerome, Rep. Prog. Phys. **54**, 351 (1991), and references therein.
[24] H. Amenitsch, S. Bernstorff, M. Kriechbaum, D. Lombardo, M. Rappolt, and P. Laggner, J. Appl. Crystallogr. **30**, 872 (1997).
[25] S. Kralj, S. Žumer, and D. W. Allender, Phys. Rev. A **43**, 2943 (1991).
[26] A. Linhananta and D. E. Sullivan, Phys. Rev. A **44**, 8189 (1991).
[27] J. Chen and T. C. Lubensky, Phys. Rev. A **14**, 1202 (1976).
[28] S. Kralj and S. Žumer, Phys. Rev. E **54**, 1610 (1996).
[29] A. Rapini and M. Papoular, J. Phys. (Paris) **30**, 54 (1969).
[30] M. Slavinec, S. Kralj, S. Žumer, and T. J. Sluckin (to be published).
[31] S. J. Singer, Phys. Rev. E **93**, 2796 (1993).
[32] P. E. Cladis and M. Kleman, J. Phys. (Paris) **33**, 591 (1972).
[33] N. D. Mermin, Rev. Mod. Phys. **51**, 591 (1976).
[34] E. B. Loginov and E. M. Terentjev, Kristallografiya **30**, 10 (1985) [Sov. Phys. Crystallogr. **32**, 166 (1987)].
[35] S. Kralj and T. J. Sluckin, Liq. Cryst. **18**, 887 (1995).
[36] W. F. Brinkman and P. E. Cladis, Phys. Today **35** (5), 48 (1982).